Penta-Hepta Defect Chaos in a Model for Rotating Hexagonal Convection

Yuan-Nan Young and Hermann Riecke

Department of Engineering Sciences and Applied Mathematics, Northwestern University, 2145 Sheridan Road, Evanston, Illinois 60208

(Received 19 September 2002; published 3 April 2003)

In a model for rotating non-Boussinesq convection with mean flow, we identify a regime of spatiotemporal chaos that is based on a hexagonal planform and is sustained by the *induced nucleation* of dislocations by penta-hepta defects. The probability distribution function for the number of defects deviates substantially from the usually observed Poisson-type distribution. It implies strong correlations between the defects in the form of density-dependent creation and annihilation rates of defects. We extract these rates from the distribution function and also directly from the defect dynamics.

DOI: 10.1103/PhysRevLett.90.134502 PACS numbers: 47.20.Bp, 47.20.Ky, 47.27.Te, 47.54.+r

Spatiotemporal chaos is at the focus of experimental [1–9] and of theoretical [10–16] research in high-dimensional dynamical systems. Most of the extensive studies have been devoted to variants of convection in thin liquid layers [3,6–8,11,14]. Detailed experimental studies have also been performed on vertically vibrated fluid layers [4] and chemical systems [2]. Theoretically, various regimes of spatiotemporal chaos of the complex Ginzburg-Landau equation have been investigated [12,16].

A striking feature of most spatiotemporally chaotic states is the appearance of defects in the pattern. In particular, dislocations have attracted great attention since they are easy to identify. Investigators have utilized their statistical, geometrical, and dynamical aspects to quantify the chaotic states in which they arise. For example, the number of dislocations (spirals) in the wave patterns governed by the complex Ginzburg-Landau equation has been found to obey Poisson-type statistics [10]. This suggests the interpretation that this system behaves as if dislocations were created randomly in pairs with a fixed probability, after which they diffuse independently throughout the system until they annihilate each other in collisions [10]. The corresponding behavior and associated distribution function have also been found in convection experiments [1,8] and in simulations of coupled Ginzburg-Landau equations for parametrically excited waves [15].

Geometric aspects of dislocations have been investigated in experiments on binary-mixture convection where the possibility to reconstruct the patterns from the dislocations has been explored [7]. In a study of a type of defect-unbinding transition, the loops formed by the dislocations' world lines in space-time have been investigated [15]. It has been found that the degree of order of the defected pattern is related to the statistics of the size of the loops [15].

The dynamical relevance of dislocations has been suggested in direct simulations of the Navier-Stokes equations of spiral-defect chaos in Rayleigh-Bénard convection [14]. The best evidence for the significance of defects as dynamical objects has been obtained by extracting their contribution to the Lyapunov dimension of the chaotic attractor [13,17].

Most of the detailed analyses of spatiotemporal chaos and of its defects have been performed in disordered patterns that are based on stripes (or rolls). Much less work has been done on spatiotemporal chaos related to other planforms [2,5,18].

In this Letter, we describe a spatiotemporally chaotic state that is based on a hexagonal pattern. Its disorder is closely tied in with the appearance of penta-hepta defects (PHDs), each of which consists of two dislocations in two of the three modes making up the hexagon pattern [19–21]. In contrast to most other systems discussed above, it is not only the instability of the background pattern that drives the chaotic state, but also the instability of the PHDs themselves. Thus, in the presence of PHDs new dislocations are created through *induced nucleation.* As a consequence, the probability distribution function for the number of defects is considerably broader than the Poisson-type distributions reported in previous studies [1,8,10]. We obtain this persistent, chaotic state in a Swift-Hohenberg–type model for rotating non-Boussinesq convection at low Prandtl numbers. While induced nucleation itself has been reported previously [22,23], without rotation it did not sustain persistent dynamics [22].

Motivated by the strong effect of mean flows and rotation on convection roll patterns [3,6], we have previously studied their effect on hexagon patterns and their PHDs using Ginzburg-Landau equations [23,24]. Since the Ginzburg-Landau equations break the isotropy of the system, they are not suited for studies of spatiotemporal chaos. In this paper, we therefore investigate a minimal extension of the Swift-Hohenberg model [25],

$$\partial_t \psi = R\psi - (\nabla^2 + 1)^2\psi - \psi^3 + \alpha(\nabla\psi)^2 + \gamma\,\hat{e}_z \cdot (\nabla\psi \times \nabla \triangle \psi) - \mathbf{U}\cdot\nabla\psi, \qquad (1)$$

$$\nabla^2\xi = \beta\hat{e}_z \cdot \{\nabla\psi \times \nabla \triangle \psi\} + \beta\delta\{(\triangle\psi)^2 + \nabla\psi \cdot \nabla \triangle \psi\},$$
$$\mathbf{U} = (\partial_y\xi, -\partial_x\xi). \quad (2)$$

The quadratic terms proportional to α and γ break the up-down symmetry $\psi \to -\psi$ and model the non-Boussinesq effects. The chiral symmetry is broken by the terms involving γ and δ; thus, to leading order these coefficients are linear in the rotation rate. The mean-flow velocity and its stream function are given by $\mathbf{U}$ and ξ, respectively, and $|\beta|$ increases with decreasing Prandtl number. We simulate (1) numerically using a parallel pseudospectral code with periodic boundary conditions. For a system size of $L = 233$ ($L = 114$), we use 256×256 (128×128) modes. To reach the chaotic states, we use mostly initial conditions consisting of an ordered hexagon pattern with a single PHD pair added; for the same mean wave numbers hexagon patterns that are only slightly perturbed (without defects) relax to stationary ordered patterns. In the chaotic regime, the patterns consist of domains of hexagons with different orientation separated by domain walls [Fig. 1(a)], where most of the PHDs are aggregated. Because of the broken chiral symmetry, the hexagon patterns in each domain precess slowly counterclockwise [26]. The corresponding space-time diagram for the temporal evolution of the radially integrated Fourier spectrum is presented in Fig. 1(b).

To identify the dislocations and PHDs, we make use of the fact that despite the disorder of the pattern its spectrum exhibits six peaks that are clearly separated most of the time and that are rotated by 120° with respect to each other [cf. Fig. 1(b)]. We demodulate the pattern using three carrier wave vectors that slowly precess along with the spectrum, $\psi = \sum_{j=1}^{3} A_j \exp[i\mathbf{q}_j(t) \cdot \mathbf{r}] +$ c.c. $+ \cdots$. Figures 2(a)–2(c) show the temporal evolution of a small section of the pattern with the roll systems making up the hexagon pattern indicated by thin lines [26].

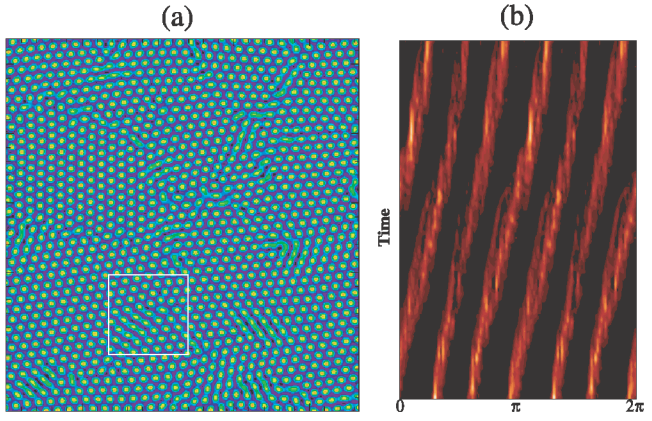

FIG. 1 (color online). (a) Snapshot of penta-hepta defect chaos for $\alpha = 0.4$, $\gamma = 2$, $\beta = -2.6$, $\delta = 0.023$, $R = 0.17$, and $L = 233$. (b) Corresponding space-time diagram of the radially integrated Fourier spectrum of the whole pattern. For a movie of the pattern and its defects, see [26].

In various experimental and theoretical investigations of stripe-based disordered patterns, the probability distribution function for the number of defects has been used to obtain a first characterization of the defect evolution [1,8,10]. Except for the case of the ordered chaotic state in [15], the probability distribution function for the number of defects was found to be close to a Poisson-type distribution, indicating that the dynamics are consistent with the simple diffusive model described above [10]. In particular, the creation rates depend only little on the defect density [8]. However, this is not the case for the penta-hepta defect chaos described here. Figure 3 gives the distribution function for the number of dislocations for two system sizes, $L = 233$ and $L = 114$ (inset), and two sets of parameter values. The symbols give the relative frequency to find n dislocation pairs in one of the three modes, whereas the dashed line gives the best fit to the squared Poisson distribution (with the same mean) corresponding to the uncorrelated dislocation dynamics [10]. Clearly, in the penta-hepta defect chaos the defect dynamics are far from uncorrelated.

A more detailed analysis of the defect dynamics reveals a strong tendency for dislocations to be created in the vicinity of already existing PHDs. This is illustrated in Fig. 2. Because of the gradient terms involving α and γ, which lead to nonlinear gradient terms in the Ginzburg-Landau equations [23], the dislocations making up the PHDs are spatially separated [22,23] [cf. Fig. 2(a)]. In addition, a PHD in modes A_1 and A_2, say, leads to a perturbation in mode A_3. For sufficiently large α and γ, the perturbation evolves into a dislocation pair in mode A_3 [marked by the splitting of the cell between the two initial dislocations in Fig. 2(a)]. The newly created dislocations then recombine with the oppositely charged dislocations in the original PHD to form two PHDs [Fig. 2(c)], which then typically move apart from each other. Such *induced* defect nucleation has been

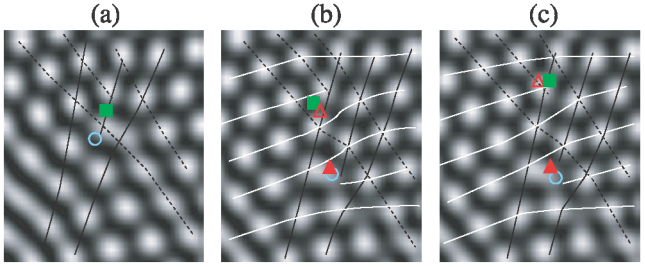

FIG. 2 (color online). Induced nucleation of dislocations. Enlargements corresponding to the box in Fig. 1(a) at times $t = 747$, $t = 759$, and $t = 760$. Thin black and white lines indicate the rolls involved in dislocations (marked by symbols).

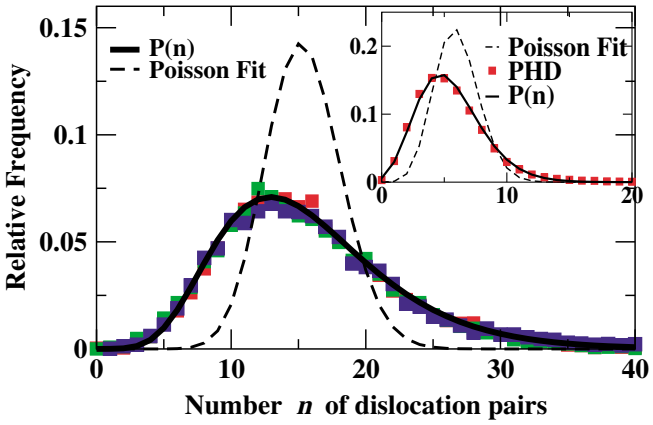

FIG. 3 (color online). Probability distribution function for the number of dislocation pairs in the pattern. Parameters as in Fig. 1. For the inset $L = 114$, $\alpha = 0.4$, $\gamma = 3$, $\beta = -5$, $\delta = 0.012$, and $R = 0.09$. Solid line is fit to (4).

found previously in coupled Ginzburg-Landau equations [22,23] and in a Swift-Hohenberg–type model without rotation or mean flow [22]. However, in contrast to the case discussed in [22], in the presence of rotation the nucleation is sufficient to sustain a precessing chaotic state.

To establish a quantitative connection between the induced defect nucleation and the defect distribution function, we consider an extension of the simple kinetic model for the defect dynamics presented in [10]. Since there are three different modes A_j and because the total topological charge of a PHD has to vanish [27], the statistics of the defect dynamics are described by a combined distribution function $\mathcal{P}_6(n_{12}^+, n_{12}^-, n_{23}^+, n_{23}^-, n_{31}^+, n_{31}^-)$ for the six different kinds of PHDs. Here n_{12}^+ denotes, for instance, the number of PHDs involving a dislocation with positive charge in mode A_1 and a dislocation with negative charge in mode A_2. In principle, there are also dislocations that are not bound in a PHD. In this kinetic model, we assume that their dynamics are fast enough to follow quickly the number of PHDs. The numerical simulations show that the densities are strongly correlated at equal times, which implies that $\mathcal{P}_6$ is strongly peaked when its six arguments are equal. Integrating out the dependence of $\mathcal{P}_6$ on five of its arguments, one therefore obtains a closed approximation for the change in $\mathcal{P}(n_{12}^+ \equiv n) \equiv \int \mathcal{P}_6 \, dn_{12}^- \ldots dn_{31}^-$ during a time interval Δt involving the creation and annihilation rates $\Gamma_n^\pm$,

$$\mathcal{P}(t + \Delta t, n) - \mathcal{P}(t, n) = \Delta t \{ \Gamma_{n-1}^+ \mathcal{P}(t, n-1) + \Gamma_{n+1}^- \mathcal{P}(t, n+1) - (\Gamma_n^- + \Gamma_n^+) \mathcal{P}(t, n) \}. \quad (3)$$

In steady state, the distribution function satisfies detailed balance, $\mathcal{P}(n+1)\Gamma_{n+1}^- = \mathcal{P}(n)\Gamma_n^+$. Assuming a fixed rate for the induced nucleation triggered by a given PHD, the rate for processes of the type shown in Fig. 2 depends linearly on the density of the PHDs involving the rolls marked by thin black lines. This process creates two dislocations which are marked by white lines and the subsequent formation of two "black-white" PHDs eliminates the original PHD. This suggests a linear contribution to the dependence of the creation and the annihilation rate on the defect density. The reverse process originates from two PHDs and therefore contributes quadratic terms. Including also the spontaneous creation of dislocations, which then form PHDs, we make the ansatz

$$\Gamma_n^- = a_1 n + a_2 n^2, \qquad \Gamma_n^+ = c_0 + c_1 n + c_2 n^2. \quad (4)$$

The steady-state solution to (3) with (4) is then given by

$$\mathcal{P}(n) = \mathcal{P}(0) \prod_{j=0}^{n-1} \frac{c_0 + c_1 j + c_2 j^2}{a_1(j+1) + a_2(j+1)^2}, \quad (5)$$

with $\mathcal{P}(0)$ determined by the normalization condition. As shown in Fig. 3, the fits of the numerical simulation results to (5) are very good for both system sizes. For $L = 114$, we obtain $c_0 = 31.8a_2$, $c_1 = 3.3a_2$, $c_2 = 0.4a_2$, and $a_1 = 5.0a_2$, confirming the strong dependence of the creation rate on the number of defects.

By tracking each dislocation from its creation to its annihilation, we can also determine the creation and annihilation rates directly from the numerical simulations. Figure 4 shows these rates for a dislocation in a given mode as a function of the number of dislocation pairs in the same mode for a system of size $L = 114$ (same parameters as in inset of Fig. 3). In principle, the rates should be given as functions of the number of PHDs involving the other modes. However, due to the finite distance between the dislocations within a PHD, the grouping of dislocations into PHDs is not always unique. Because the numbers of dislocations in the three modes are strongly correlated, taking the number of dislocations in the same mode provides a good approximation. The large scatter in the data for larger defect numbers is due to the lack of statistics for events of that kind (cf. inset of Fig. 3). Similarly, there are only few events with few defects. Clearly, in the intermediate range of n, not only the annihilation rate but also the creation rate depends strongly on the defect number.

To connect the directly measured rates with the distribution function (4), the solid curves in Fig. 4 give the creation and annihilation rates as determined from fitting the distribution function for the defect number using the form (3). For this comparison, the overall time scale (i.e., a_2) is adjusted to fit the time scale of the simulations. The rates inferred from Fig. 3 agree quite well with the directly measured ones over the statistically reliable range of n and confirm the interpretation of the distribution function's deviation from the squared Poisson distribution.

The creation rate for dislocations does not vanish for $n = 0$, i.e., when no PHDs are present. This indicates the

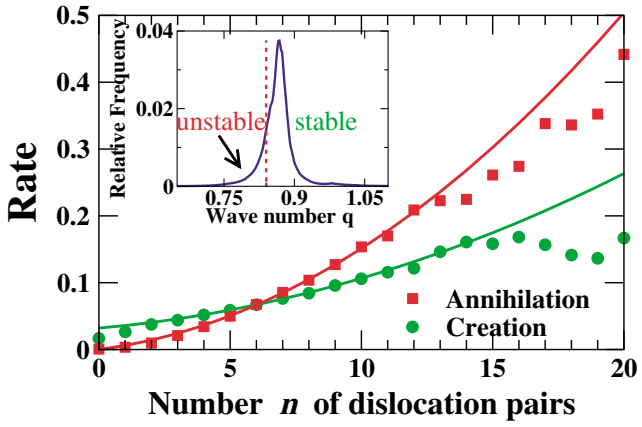

FIG. 4 (color online). Creation (squares) and annihilation (circles) rates of dislocations as a function of the number of dislocation pairs in the same mode. Parameters as in inset of Fig. 3 ($L = 114$). Inset: Wave number distribution function with stability limit for hexagons according to weakly nonlinear theory (dashed).

spontaneous creation of dislocation pairs directly from an instability of the hexagonal pattern despite the fact that the mean wave number of the pattern is inside the stability balloon. However, the distribution function for the local wave number (inset of Fig. 4) shows that in the chaotic state the distribution function extends noticeably beyond the low-q stability limit, as determined by a weakly nonlinear analysis of (1). This suggests that some dislocation pairs are created through a sideband instability in regions where the local wave number is low.

In conclusion, in a model for rotating non-Boussinesq convection we have identified a spatiotemporally chaotic state that is dominated by the dynamics of penta-hepta defects of the underlying hexagon pattern. In contrast to previously analyzed chaotic states, which are stripe based, the defect statistics of this penta-hepta chaos indicate strong correlations between the defects. We identify the origin of the correlations as the induced nucleation of dislocations due to the presence of penta-hepta defects. From the defect statistics, we extract the dependence of the creation and annihilation rates of defects on the defect density and find good agreement with the rates measured directly by following the defects in the simulations. In ongoing direct simulations of the Navier-Stokes equations for rotating non-Boussinesq convection, we have found cases of induced nucleation of dislocations [28].

We wish to acknowledge useful discussions with K. E. Daniels, A. Golovin, A. Nepomnyashchy, and L. Tsimring. This work was supported by grants from the Department of Energy (DE-FG02-92ER14303), NASA (NAG3-2113), and NSF (DMS-9804673). Y. Y. acknowledges computation support from the Argonne National Labs and the DOE-funded ASCI/FLASH Center at the University of Chicago.

[1] I. Rehberg, S. Rasenat, and V. Steinberg, Phys. Rev. Lett. **62**, 756 (1989).
[2] Q. Ouyang and H. Swinney, Chaos **1**, 411 (1991).
[3] S. Morris, E. Bodenschatz, D. Cannell, and G. Ahlers, Phys. Rev. Lett. **71**, 2026 (1993).
[4] A. Kudrolli and J. Gollub, Physica (Amsterdam) **97D**, 133 (1996).
[5] M. Dennin, G. Ahlers, and D. S. Cannell, Science **272**, 388 (1996).
[6] Y. Hu, W. Pesch, G. Ahlers, and R. E. Ecke, Phys. Rev. E **58**, 5821 (1998).
[7] A. La Porta and C. M. Surko, Physica (Amsterdam) **139D**, 177 (2000).
[8] K. E. Daniels and E. Bodenschatz, Phys. Rev. Lett. **88**, 034501 (2002).
[9] E. Bodenschatz, W. Pesch, and G. Ahlers, Annu. Rev. Fluid Mech. **32**, 709 (2000).
[10] L. Gil, J. Lega, and J. Meunier, Phys. Rev. A **41**, 1138 (1990).
[11] W. Decker, W. Pesch, and A. Weber, Phys. Rev. Lett. **73**, 648 (1994).
[12] H. Chaté and P. Manneville, Physica (Amsterdam) **224A**, 348 (1996).
[13] D. A. Egolf, Phys. Rev. Lett. **81**, 4120 (1998).
[14] D. A. Egolf, I. V. Melnikov, W. Pesch, and R. E. Ecke, Nature (London) **404**, 733 (2000).
[15] G. D. Granzow and H. Riecke, Phys. Rev. Lett. **87**, 174502 (2001).
[16] I. S. Aranson and L. Kramer, Rev. Mod. Phys. **74**, 99 (2002).
[17] M. Strain and H. S. Greenside, Phys. Rev. Lett. **80**, 2306 (1998).
[18] E. Hernández-Garcia, M. Hoyuelos, P. Colet, and M. San Miguel, Phys. Rev. Lett. **85**, 744 (2000).
[19] S. Ciliberto, P. Coullet, J. Lega, E. Pampaloni, and C. Perez-Garcia, Phys. Rev. Lett. **65**, 2370 (1990).
[20] J. Millán-Rodríguez, C. Perez-Garcia, M. Bestehorn, M. Neufeld, and R. Friedrich, Chaos **4**, 369 (1994).
[21] L. Tsimring, Phys. Rev. Lett. **74**, 4201 (1995).
[22] P. Colinet, A. A. Nepomnyashchy, and J. C. Legros, Europhys. Lett. **57**, 480 (2002).
[23] Y.-N. Young and H. Riecke, Physica (Amsterdam) **176D**, 107 (2003).
[24] Y.-N. Young and H. Riecke, Physica (Amsterdam) **163D**, 166 (2002).
[25] M. Fantz, R. Friedrich, M. Bestehorn, and H. Haken, Physica (Amsterdam) **61D**, 147 (1992).
[26] See EPAPS Document No. E-PRLTAO-90-021310 for movies of the temporal evolution of the pattern and of its defects. A direct link to this document may be found in the online article's HTML reference section. The document may also be reached via the EPAPS homepage (http://www.aip/org/pubservs/epaps.html) or from ftp.aip.org in the directory /epaps/. See the EPAPS homepage for more information.
[27] M. Rabinovich and L. Tsimring, Phys. Rev. E **49**, 35 (1994).
[28] Y.-N. Young, H. Riecke, W. Pesch, and V. Moroz (unpublished).